


Review

Review on Electrical Impedance Tomography: Artificial Intelligence Methods and its Applications

Talha Ali Khan * and Sai Ho Ling 

School of Biomedical Engineering, University of Technology Sydney, Ultimo, NSW 2007, Australia;
steve.ling@uts.edu.au

* Correspondence: talha.khan@uts.edu.au

Received: 13 February 2019; Accepted: 23 April 2019; Published: 26 April 2019



Abstract: Electrical impedance tomography (EIT) has been a hot topic among researchers for the last 30 years. It is a new imaging method and has evolved over the last few decades. By injecting a small amount of current, the electrical properties of tissues are determined and measurements of the resulting voltages are taken. By using a reconstructing algorithm these voltages then transformed into a tomographic image. EIT contains no identified threats and as compared to magnetic resonance imaging (MRI) and computed tomography (CT) scans (imaging techniques), it is cheaper in cost as well. In this paper, a comprehensive review of efforts and advancements undertaken and achieved in recent work to improve this technology and the role of artificial intelligence to solve this non-linear, ill-posed problem are presented. In addition, a review of EIT clinical based applications has also been presented.

Keywords: electrical impedance tomography; artificial intelligence methods; health care; imaging technique

1. Introduction

Electrical impedance tomography (EIT) assesses the human body's internal electrical characteristics by taking measurements from the external surface of the body [1]. Usually, this is done by injecting the current into the object through electrodes located on its surface, and the corresponding voltages are measured. The aim here is to reconstruct the electrical permittivity and conductivity distributions inside the object from the knowledge of the measured electrode voltages and applied current patterns by solving an inverse problem [2]. In EIT, any substantial changes in impedance would only result in a minor change at the surface which makes the solution of the inverse problem a highly challenging task [3].

EIT has a lower imaging resolution in comparison to magnetic resonance imaging (MRI) and computed tomography (CT). EIT is entirely non-invasive and carries out a radiation-free imaging modality. EIT has an advantage over the other imaging techniques such as its portability, low-cost, and faster imaging capabilities. EIT proves to be efficient when producing an impedance map of the inside of a human skull even for areas where ultra-sonic techniques do not prove to be sufficient. The initial usage of EIT was reported 100 years ago in the study of geological surveys [4]. Others have used a similar technique for the detection of air bubbles in process pipes or for monitoring the pipe flows, which today is known as industrial process tomography. In 1978 for the first time, Henderson and Webster published impedance images of human tissues [5]. They created a transmission map from current-voltage data with 100 electrodes formed into a rectangular array by fixing it on one side of the human chest while earthing the opposite side of the body using a single large electrode. On the object's surface, using electrical measurements, EIT seeks to reconstruct a resistivity distribution. In the resulting image, the low conductivity areas would correspond to the lungs. Unlike X-ray tomography [6], in EIT the current paths and the equipotential surfaces are the functions of the unknown resistivity distribution.

2. Imaging Modalities of Electrical Impedance Tomography (EIT)

EIT image reconstruction techniques can be divided into three sub-categories, frequency difference, absolute imaging, and time difference. All these techniques are reliant on a computer-based model (called the mesh) of the subject under analysis, that is used to simulate the estimated electric potential distributions for the injected current patterns. A Jacobian matrix is required for all the reconstruction techniques that are calculated depends upon the forward solutions. The Jacobian matrix indicates the variations in conductivity to fluctuations in the measured voltages by linearizing the computer model and notifies the imaging algorithms of the search direction. The image results will be good if the mesh is closer for computation.

2.1. Absolute Imaging

The simplest method to produce an image from EIT measurements is that within the measured object plot the measured voltages directly to a conductivity distribution. In absolute imaging at any point in time, images can be produced without the need for reference calculations.

2.2. Time-Difference

The time-difference imaging technique works on the principle that it estimates the differences between the measured voltages at time t to a reference calculation attained at time t_0 and states the difference in voltages by a variation in conductivity between these two points.

2.3. Frequency-Difference

The basic principle on which multi-frequency EIT (MFEIT) works is that impedance of every tissue has a unique frequency spectra and it allows the one-shot imaging deprived of the disadvantages that absolute imaging encounters. Spectral data can be reconstructed and achieved by calculating various frequencies at the same time or in rapid sequence. Similarly to time-difference, one measurement is obtained as a reference, other is taken at a different frequency, and then it will be reconstructed by inverting the Jacobian matrix.

3. How EIT Works

The EIT works by using different processes starting from electrical properties of tissues to highlight the tissue state to characterize diagnostically valuable information. The following are the steps involved to represent how EIT works.

- i Contrasting the electrical properties of the tissues.
- ii EIT measuring devices and electrodes positioning.
- iii Data collection and solving the forward problem.
- iv Image reconstruction (inverse problem).
- v Image processing on EIT image.
- vi Taking valuable information for the diagnosis of disease from EIT image.

In this paper, the focus will be on the steps of solving the forward and the inverse problem.

3.1. Forward Problem and Data Collection

The first step for solving the forward problem is to collect data from the subject's body area under examination. A common EIT system uses a number of electrodes that are connected to the exterior surface of the patient body area under monitoring or examination. Current or voltage is applied to the body and the resulting current or voltage is calculated. Typically, the current is applied from an alternating current (AC) source to a few electrodes and the measuring voltages are calculated to form the remaining electrodes.

3.1.1. Types of Current Injection Patterns

There are many types of configurations used for applying current and calculating the resulting voltages but most common is the pair drive configuration. The pair drive configuration consists of a single current source that is connected to the electrode pairs which is used to inject current into the medium and the resulting potential is calculated from the rest of the electrodes. After obtaining the first measurement, the AC source is moved to the other pair of electrodes and the process continues until all the measurements have been completed. The other configuration is the multiple drive configuration in which the current is applied to the medium by using more than two electrodes simultaneously. It is expensive and complex as compared to the pair drive configuration that uses only one AC source. Some of the current injection patterns that are used for the 2D configurations are as follows:

- Adjacent Current Pattern
- Cross Current Pattern
- Opposite Current Pattern

3.1.2. Finite Element Method (FEM)

The forward problem can be solved analytically for simple shapes. For the complex medium, it is necessary to discretize the whole domain into small elements called meshes. For the discretized medium, there are many numerical techniques present to solve this forward problem. Some of these methods include finite volume and finite difference approaches that generally need regular grids. However, the drawback of these methods is that they need a regularity requirement while representing curved structures. The finite element method (FEM) is usually used for EIT applications. The advantage of the FEM is that it does not need any regularity of the discretization. The increase in the number of elements in the meshes will result in the FEM solution moving towards the real solution of the partial differential equation. To formulate the FEM problems, three types of approaches are usually used.

- Direct Method
- Variational Method
- Method of Weighted Residuals (MWR)

3.2. Inverse Problem

In EIT, the approximation of the conductivity distribution from the calculated data is called the inverse problem. The inverse problem is an ill-conditioned problem, which means that a slight variation in the measured data causes a huge impact on image reconstruction. As a result, in terms of the existence of noise, the inverse problem is highly unstable in nature. In addition, for the isotropic conductivities, the solution must be unique and the information for boundary condition is required. Due to the anisotropic nature of human tissues, the implementation of the many electrodes create practical complications and, for this reason, it is not viable to reconstruct the conductivities exactly. Therefore, a stable reconstruction approach is required that can obtain an approximate solution. In EIT, the inverse problem is an ill-posed problem but through regularization by introducing prior information, and it is possible to transform it into a well-posed problem.

Methods for Solving the Inverse Problem

There are many approaches to solve the inverse problem with many of these techniques which are adding a priori information through a method known as regularization. The image reconstruction algorithms are divided into two categories deterministic and stochastic. The stochastic method depends upon probabilistic statistical reasoning whereas; the deterministic method is further be categorized into non-linear and linear techniques.

4. Solving the Inverse Problem

Hadamard defined that for vector spaces X and Y such that $T: X \rightarrow Y$. For a given general problem $T(x) = y$ where x is unknown. This problem is defined as the well-posed problem only if it satisfied the following conditions [6].

- The inverse mapping is continuous.
- The solution does exist.
- The solution is unique.

By contrast, if the problem does not satisfy any of the conditions as mentioned above the problem is an ill-posed or ill-conditioned problem. For solving $T(x) = y$ for the unknown x it is called as the inverse problem. It is generally used when T is continuous and exists for evaluating T such that the forward problem is a classical or least well-known problem. The term inverse problem is only used for an ill-posed problem according to the Hadamard conditions.

EIT is an ill-conditioned problem since there is not only a unique solution (image reconstruction) of this inverse problem for the given potential border distribution. Rolnik et al. have concluded that in EIT inverse problem the image generated is not always consistent or well defined [7]. As a result, different methods are adopted to solve the EIT inverse problem as an optimization problem. The objective is to reduce the relative error between the calculated border potential of the solution candidate and measure border potential of an object. Many researchers have worked on different artificial intelligence methods and evolutionary computational techniques to solve this inverse problem.

In the beginning, many linear algorithms for image reconstruction have been proposed including the sensitivity matrix technique, equipotential back projection, and regularization approach. On the other hand, the linear hypothesis is effective only if the perturbation from the linearization point is slightly small in which there are no large areas where conductance varies not too much from the background. Many reconstruction approaches have been used for EIT, the standard method is the use of regularized Newton-type techniques. The application of this method to solve the inverse problem is quite clear since the EIT problem is non-linear so the first step is to linearize it since the linear problem is an ill-posed problem, and therefore, regularize it; the linear approximation cannot reconstruct complex geometries or large contrasts so the process must be applied iteratively. The most common non-linear Newton-type method is the Newton–Raphson method. This technique works by searching the conductivity distribution that reduces the difference between applied potentials and the calculated potential from the forward problem by finite element method. The drawback of this algorithm is that it is computationally complex, requires numerous orders of magnitude and computational time is high as compared to the linear methods.

These non-linear methods give good results if the hypotheses about the problem are simplified. A Neural Network (NN) is also used to solve the linear problem as compared to linear algebraic methods. This is because the problem is ill-posed. The advantage of using the NN is that the inverse of the matrix is taken directly from the finite element method and Signal to Noise Ratio (SNR) is achieved without any initial hypotheses and calculations. However, the training of the NN is highly affected due to the ill-conditioning of the problem. During the training, the NN responds to training patterns near the boundary of the domain and at the center, it responds to the training patterns only when the performance on the boundary is approximately optimal. Moreover, the under-determination indicates that spatial resolution is poorer to the size of the training patterns [8]. As a result, the NN can never replicate the training patterns precisely, and the error will never tend to zero, but will only decrease to a fraction of the initial error. However, the EIT image reconstruction method is an inverse, ill-posed and ill-conditioned problem that results in high computational cost and image with low spatial resolution.

Another possible way to solve the EIT problem is by considering it as an optimization problem that can be solved by using different methods of evolutionary computation. This works by reducing the root mean square relative error between the simulated and measured electrical potentials. In this paper, different methods have been summarized to highlight how different authors used these approaches to solve the inverse problem. Tables 1–4 highlight the use of the particle swarm optimization (PSO)

algorithm, various versions of NN and many other algorithms for solving the inverse problem. In Table 1, different versions of the PSO methods are used to solve the inverse problem. Some authors used the standard PSO, hybrid versions of PSO and others used modified forms as well. The results achieved from PSO demonstrated good performance when compared to the linear algorithms for solving the inverse problem in terms of image resolution, computational cost and time. From the literature review, it is also noticeable that PSO shows good convergence than the other EC methods.

Table 1. Overview of papers using particle swarm optimization (PSO) approach for solving the Inverse problem.

Reference	Algorithm	Remarks
Zhang et al. [9]	MPSO MNR	Used Modified Particle Swarm Optimization with Modified Newton–Raphson (MPSO-MNR) algorithm and analyzed the effect of noise on the algorithm for EIT. The results show the proposed method reconstructed the resistivity distribution within a few iterations.
Wang et al. [10]	MPSO	Modified PSO is used to reconstruct the conductivity distribution for EIT images; the results demonstrated better performance and finds the object in the circular medium.
Allan et al. [11]	CRPSO-NBS	Various versions of PSO with different initialization approaches are used to compare the effectiveness of the proposed Chaotic Ring-Topology PSO with Non-blind Search (CRPSO-NBS) for optimizing the relative error of reconstruction. The proposed method gives better results in a few iterations as compared to other methods.
Peng et al. [12]	PSO with RBF Neural Network	RBF NN network’s connection weights are optimized by using PSO. The PSO-RBF enhanced the quality of the reconstructed image. The method is also useful for calculating the resistivity distribution.
Weili et al. [13]	GBPA and PSO	A new excitation mode is presented for a generalized back-projection algorithm (GBPA). PSO is used to optimize the injection configuration. Imaging results achieved for the optimized configuration is compared with the conventional method.
Ruilan et al. [14]	PSO-tGN	A hybrid version of PSO and Gauss-Newton algorithm is used. PSO is used to achieve the EIT electrical impedance distribution and Gauss-Newton algorithm is then used to solve the problem iteratively.
Kumar et al. [15]	PSO-EIT	PSO-EIT is used to enhance image reconstruction for brain images. The results of the PSO-EIT is compared with the Modified Newton Raphson and Genetic Algorithm in terms of signal to noise ratio and relative error.
Chen et al. [16]	PSO	An adaptive PSO is combined with the modified Newton Raphson Algorithm to enhance the EIT image quality. The results obtained showed better convergence and higher spatial resolution of the image as compared to the Newton–Raphson algorithm.
Martin et al. [17]	ANN-PSO	PSO is used to improve the training of the artificial neural network (ANN) for solving the EIT inverse problem.
Choi et al. [18]	PSO-NN	PSO is used for the training of NN to solve the limitations in the forward problem of the EIT.
Lee et al. [19]	PSO	PSO is combined with the Gauss-Newton method to visualize the two-phase flow for the electrical resistance tomography.
Lin et al. [20]	SAP	Simulated Annealing particle swarm optimization (APSO) is combined with least squares support vector machines (LS-SVM) for the image reconstruction of electrical capacitance tomography (ECT) by searching the optimized resolution.
Umer et al. [21]	PSO	PSO is used to solve the EIT forward problem by assuming that the smooth elliptic medium boundary information is missing. PSO is used to iteratively look for the boundary conditions by reducing a cost function.
Chen et al. [22]	PSO	PSO is used to solve the inverse EIT problem instead of formulating the Jacobian matrix. It is compared with the Newton–Raphson (MNR) algorithm and better results are obtained in terms of image resolution.
Hui et al. [23]	PSO	By using, the method of the moment in a circular configuration for a homogeneous 2D domain is studied and PSO is used to reconstruct the real object. Assuming the analysis as noise free and several other constraints are also applied.
Sun et al. [24]	APSO	An adaptive particle swarm weight is used for the gray boundary compensation algorithm for electrical capacitance tomography. The introduction of the average absolute speed and ideal speed in the swarm is used to adjust the parameters of the PSO that in turn used to adjust for the gray border around the image.
Shi et al. [25]	PSO and RBF Neural Network	A new hybrid method based on the PSO and RBF NN is used for optimizing the parameters of ECT sensors. The results achieved demonstrated good quality of the reconstructed image.

Table 2 shows the use of the NN for solving the inverse problem; different methods have been applied along with NN to solve the inverse problem. Some authors used PSO for training the weights of the NN while others used radial basis function NN for solving the problem. The results obtained from the NN show good image resolution as compared to the Newton methods and Tikhonov regularization. However, the drawback of using the NN leads to computational cost, and a large amount of data is used to train the NN.

Table 2. Overview of papers using the neural network approach for solving the inverse problem.

Reference	Algorithm	Remarks
Zhang et al. [26]	NN	An algebraic NN (Neural Network) is used for the reconstruction of the electrical resistance tomography. It converts image reconstruction into a problem of solving strictly linear equations. The approach showed good convergence and small reconstruction error.
Cai et al. [27]	BP-NN	A neural network is used to replace the conventional back-projection algorithm for the image reconstruction of the electrical capacitance tomography images. The improved backpropagation algorithm trains a two-layer perceptron network and it demonstrated better image resolution.
Martin et al. [17]	ANN-PSO	PSO is used to improve the training of the artificial neural network (ANN) for solving the EIT inverse problem.
Choi et al. [18]	PSO-NN	PSO is used for the training of NN to solve the limitations in the forward problem of the EIT.
Zhang et al. [28]	RBF NN	RBF neural network is used for the image reconstruction of the electrical capacitance tomography. The modified NN improved the finite element plotting pattern, data normalization, and input layers.
Wei et al. [29]	RBF NN	A radial basis function neural network (RBF-NN) is used for the image reconstruction of the electrical resistance tomography. The algorithm compared with the other image reconstruction algorithms and shows high convergence and accuracy.
Li et al. [30]	RBF NN	RBF neural network is used for the image reconstruction of the Electrical Capacitance Tomography (ECT). For optimizing the centers and widths of the hidden units of RBF networks, an adaptive genetic algorithm is used. Training for the weights of the neural network is performed by using Tikhonov regularization. The method has increased image quality.
Xiao et al. [31]	BP NN	A neural network is used for the two-phase flow electrical capacitance tomography problem.
Chen et al. [32]	BP Neural Network and Median Filter	BP neural network is used for the image reconstruction of the electrical capacitance tomography. The method is used to achieve the conditions of flow regime identification and emphatically examined median filter to recognize image improvement.
Zhao et al. [33]	RBF NN	RBF neural network for eight electrodes electrical capacitance tomography system is presented. The training of the network is performed by using the genetic algorithm merge with the nearest neighbor clustering method.
Bai et al. [34]	RBF NN and Wavelet Transform	A RBF-NN algorithm is used to achieve the conditions of flow regime identification for image reconstruction for the ECT system. An adaptive wavelet filter image reconstruction algorithm depends upon RBF that belongs to a space-frequency analysis technique appropriate for image feature enhancement is studied to improve the reconstruction precision. The algorithm gives good quality of reconstructed images, noise reduction, and edges detection.
Yan et al. [35]	RBF NN	RBF neural networks are used for the sixteen-electrode ECT system. It is used to transform the electrode capacitance measurements into the permittivity distributions in the image domain. The number of hidden nodes in RBF-NN are determined by using a maximal matrix element approach and the center width of the RBF function is determined by using the nearest neighbor-clustering method. The image reconstructed is better in quality than the linear back projection algorithm.
Zhao et al. [36]	RBF NN	RBF neural network is used for the eight-electrode ECT system. Training of the network is performed by combining genetic algorithm along with nearest neighbor clustering algorithm.
Xiao et al. [37]	Multi-layer NN	A two multi-layer neural network model for image reconstruction of two-phase flow electrical capacitance tomography is used.
Wang et al. [38]	Wavelet Neural Network (WNN)	Wavelet neural network is used for ECT image reconstruction. The principal component analysis technique is used to minimize the dimension of the input vectors. The transfer functions of the neurons in the WNN are wavelet base functions that are determined by retracting and translation factors. The BP algorithm performs training of the WNN also self-adaptive learning rate and momentum coefficient are used to speed up the learning procedure.
Tomasz et al. [39]	Neural Networks and Deep Learning	Deep Learning methods along with the NN are used for the electrical impedance tomography. A multilayer perceptron neural network is used to detect the position of the object.

Table 2. Cont.

Reference	Algorithm	Remarks
Liang et al. [40]	Feedforward NN	A feed-forward neural network is used to solve the forward problem of ECT sensor system. The training of the NN is performed by using the experimental data. NN has also been combined with a modified iterative linear back projection reconstruction algorithm. The method showed improved results than Landweber reconstruction technique with LFP forward solver.
Sikora et al. [41]	NN	Two artificial neural networks (ANN) reconstruction approaches are used for EIT. The first method is used for ANN learning by using electric potential vectors achieved from the forward problem. The second method consists of a feed-forward multilayered neural network is used for the circuit representation of the finite element discretization.
Aki et al. [42]	Bayesian NN	Principal component projection is used to transform the EIT inverse problem into a reduced dimension problem. MLP BNN is used to solve the reduced problem. This methodology comprises a double regularization effect first because of using neural networks that learn the distribution of feasible solutions from the training data and second due to solving the inverse problem in the eigenspace.
Jan et al. [43]	ANN	A multi-region boundary element method (BEM) is used for determining the distribution of potential in the breast model in an EIT problem. A novel method based on the principal component analysis and NN is used for solving the inverse problem.
Fan et al. [44]	MLFF-NN	A hybrid version of the multilayer feed-forward neural network (MLFF-NN) and analog Hopfield network is used for ECT reconstruction. The forward problem is solved by using MLFF-NN and the inverse problem is solved by analog Hopfield network based on a neural-network multi-criteria optimization image reconstruction technique (HN-MOIRT).
Luis et al. [45]	ANN Ensemble	ANN is used for solving EIT inverse problem for the cardiac ejection fraction.
Robert et al. [8]	NN	A reconstruction algorithm is used for EIT that depends upon the NN approach that computes a linear approximation of the inverse problem directly from finite element simulations of the forward problem.
Raiwa et al. [46]	RBF NN	RBF Neural Networks is used for image reconstruction of EIT images. Training is performed by using MATLAB toolbox by using the simulated voltage measurements and EIDORS difference reconstruction element values.
Radek et al. [47]	Radial Basis NN	Radial basis neural networks (RBNN) and Hopfield neural networks (HNN) for image reconstruction of EIT images are used. The experiments result are compared with the Gauss-Newton method and show a better quality image.
Xin et al. [48]	Back Propagation NN	Backpropagation NN algorithm is used to solve the EIT inverse problem.

Table 3 shows the use of the genetic algorithm (GA), different modified versions of which are used for solving the inverse problem. It shows that the GA demonstrated good results for reconstructing static images than the modified Newton-type methods.

Table 3. Overview of papers using a genetic algorithm (GA) for solving the inverse problem.

Reference	Algorithm	Remarks
Xiao et al. [49]	IGA	An improved genetic algorithm (IGA) is used for the forward problem in electrical resistance tomography for numbering of the nodes in the finite element meshes. It helps to reduce the memory capacity for the computational data.
Chen et al. [50]	GA	Genetic algorithm (GA) is used for the two-phase flow electrical capacitance tomography image reconstruction. The results show that the section image of two-phase flow is reconstructed with the higher resolution.
Olimi et al. [51]	GA-EIT	GA is used for the EIT inverse problem for the reconstruction of the static images. The method is compared with the modified Newton-Raphson and the double-constraint method and the images obtained are of good quality.
Kim et al. [52]	GA	GA is used for the static EIT inverse problem. The method is validated by simulation of the 32 channels synthetic data and the images reconstructed have better resolution than modified Newton-Raphson algorithm.
Paulo et al. [53]	GA	An error function is formulated for the reconstruction problem that is used to measure the changes between the actual internal and prospective contrast distribution and find out its minimum by using a genetic algorithm.
Grazieli et al. [54]	HPGA	A priori information is added in the GA for the global minimum search for solving EIT problem. Hybrid Parallel Genetic Algorithm (HPGA) and a priori Information give good result for global minimum search than without Priori Information.
Kuo et al. [55]	GA	GA is used for reconstructing the electrical impedance image. The impedance image reconstruction is solved as a minimization problem. The cost function is defined as the errors between the measured and estimated boundary voltages in the least square.

Table 4 elucidates the use of miscellaneous algorithms for solving the EIT problem. It is shown that different methods other than EC techniques and NN were used previously. These algorithms are used for solving both the inverse and forward problems for the electrical tomography problem. Besides, in reconstructing the image some algorithms are used to measure the next states as the change in impedance is so fast while others solve the inverse problem as an optimization problem.

Table 4. Overview of papers using various other algorithms for solving Inverse problem.

Reference	Algorithm	Remarks
Chen et al. [56]	Landweber iteration algorithm	Landweber iteration algorithm is used for the ECT image reconstruction. Tikhonov regularization is used instead of the Linear Back Projection algorithm.
Xu et al. [57]	Levenberg–Marquardt	Levenberg–Marquardt Algorithm merges the features of the steepest descent algorithm and Gauss–Newton algorithm to solve the inverse ECT problem. Instead of using the Jacobian matrix for solving the inverse problem it uses the sensitivity coefficient matrix.
Hu et al. [58]	Iterated Tikhonov Regularization	A new operator is used for the standard Tikhonov algorithm. The new method improves the speed and accuracy of the standard method.
Liu et al. [59]	Support Vector Machine	An image reconstruction algorithm is used based on the support vector machine to reconstruct the ECT images instead of BP reconstruction algorithm.
Sun et al. [60]	Fletcher–Reeves algorithm	The ill-posed equation of image reconstruction transform into minimization problem function, the function is solved later by using the Fletcher–Reeves algorithm (FR)
Lei et al. [61]	Iteration algorithm based on 1-norm	Image reconstruction algorithm based on the 1-norm stabilizing is used. The image reconstruction problem is transformed into an optimization problem.
Han et al. [62]	Active Filter Linear Back Projection Method	Active filter linear back projection algorithm is used for the reconstruction of ECT images.
Kim et al. [63]	Extended Kalman Filter	A reconstruction algorithm that depends upon the modified extended Kalman filter technique is used for the reconstruction of EIT images. The algorithm is capable to observe sudden variations in the impedance distribution and perform better than the conventional Kalman filter method.
Trigo et al. [64]	Extended Kalman Filter	Extended Kalman filter is used to solve the EIT inverse problem by estimating the conductivity distribution for controlling the level of pressure and air volume for patients at ventilation.
Dos et al. [65]	Fish School Search and differential evolution	Fish school search and differential evolution algorithms by using a non-blind search approach are used to solve the EIT inverse problem. A phantom of the circular section is used to regenerate the images by placing the object at different positions. Both the algorithms give faster convergence.
Ying et al. [66]	Differential Evolution Algorithm	Differential evolution algorithm is used to solve the EIT inverse problem of a brain portion based on the real head model by estimating the cost function that is obtained by solving the forward problem.
Kaipio et al. [67]	Kalman filter	Since the variations in impedance are so swift that the information is lost, therefore Kalman filter is used to estimate the states.
Liu et al. [68]	Sparse Bayesian learning	Sparse Bayesian learning method is used to reconstruct sequential EIT frames with an improved resolution by using spatiotemporal prior.
Jia et al. [69]	Sparse Bayesian Learning	A novel reconstruction algorithm based within the framework of sparse Bayesian learning is used to obtain the high-resolution EIT images. Structure-aware priors are imposed on the learning process to include prior knowledge. As a result, the method conserves the shape information at a low signal-to-noise ratio and eludes the time-consuming parameter tuning process.
Wu et al. [70]	SA-SBL	Structure-aware sparse Bayesian learning (SA-SBL) method is used for reconstruction of three-dimensional conductivity distribution by using EIT approach. In addition to enhancing, the large-scale 3D learning process an effective method depends upon the approximate message passing is also presented.
Yang et al. [71]	BSBL	Block sparse Bayesian learning (BSBL) is used for conductivity distribution reconstruction in a phantom. The BSBL reconstruct the noisy conductivity variation maps with block sparsity, both in spatial resolution and robustness features.
Giza et al. [72]	Bell functions approximation	An objective function with bell function parameters has been used to approximate the conductivity distribution inside the body. It decreases the computational time and helps to simplify the reconstruction process. It shows better performance as compared to the Gaussian function.

5. EIT Clinical-Based Applications

Recently, different types of medical imaging applications with EIT have investigated, such as gastric emptying measurement, brain imaging, breast imaging, lung imaging, and osteography.

5.1. Gastric-Emptying Measurement

In Gastric measurement, impedance methods can be used to examine stomach emptying as meal changes the resistivity in the upper abdomen of the body. The gastric wall conductivity is about 5 m Siemens cm^{-1} [73]. Emptying can be calculated depending upon the meal being either less or more conductive, as this can be noted as a difference in an EIT image. On the other hand, conductivity can rise if the level of the conductivity is low in a meal by the secretion of gastric juices and, therefore, can complicate the measurement of the EIT variations, as secretion cannot be differentiated from emptiness. Acid secretion can be reduced by using Cimetidine but ethically it is not allowed to use this medicine because, for instance, physiology of the stomach of the young children can be affected [74]. Researchers have obtained steady emptying curves by using a comparatively conductive meal to overcome this problem.

The management of certain gastric disorders is the most important test after eating for measuring the rate of emptying of the stomach. Gamma scintigraphy is the most common technique for the calculation of gastric stenosis: the rate of gamma emission after the patient takes a radiolabelled test substance is calculated in the area around the stomach. This may be significant as the radiation dose is also important when making regular check-ups in adults or examining infants. Intubation techniques may be used in these cases. For instance, in the case of studying dye dilution, to supply a small quantity of material having string coloring the patient swallows a nasogastric tube. The nasogastric tube can extract the samples of stomach contents. The volume of the stomach at any point of time can be found from the ratio of the quantity of the dye delivered to its concentration in the gastric sample. Mangnall et al. [75] did a comparison for EIT between the dye dilution method and isotope scintigraphy, which needs gastric intubation. The experiment was conducted on 19 volunteers whereby 16 electrodes in a circular array were placed at an equal distance from each at the level of the eighth costal cartilages. To reduce acid secretion, Cimetidine was given. The outcomes of the experiments highlighted that the profiles of gastric emptying that Electrical Impedance Tomography gives are similar to the other methods that are applied. The advantage of it that on the same patient, numerous another experiment can be done and the technique is also non-invasive as there are no known threats. Authors in [76] have performed experiments on 18 infants and concluded that after taking the conductive drink the time for the stomach volume is reduced by half. There are more emptying times in infants with pyloric stenosis as compared to infants that do not have this. The resistivity of the stomach area is affected due to its size and content [77]. Wang et al. in [78] have studied the application of EIT to calculate gastric acid secretion. Standard intubation test was conducted on 19 healthy people. Stimulated acid output (SAO) and basal acid output (BAO) (millimoles per hour) were calculated after and before pentagastrin. They have concluded that the likely change of gastric impedance can be beneficial as a non-invasive test for calculating gastric acid secretion.

5.2. Head Imaging

Brain imaging is a challenging clinical task. The brain tissues impedance increases drastically during cerebral ischemia. To calculate the severity of the stroke a non-invasive technique is required. Holder has performed different experiments with both cranial and intracranial electrodes on anesthetized rats [79] and obtained images of cerebral ischemia. He carried out a research review on EIT. By using electrodes, he stated that the visible surface of the cerebral cortex of the animals is very effective over milliseconds associated to neuronal depolarization in imaging evoked impedance variations and over a number of seconds for those linked to metabolic recovery procedures. The deviations have been observed during evoked responses and cortical spreading depression [80]. He believed that in the near future the process would be used for brain imaging for humans too. For static imaging of the head, the authors have developed, studied and compared three EIT techniques. Based on the real head model for impedance reconstruction of the head section, they applied these techniques to a 2D model. The results validated that the amalgam of the improved Newton–Raphson, and differential evolution algorithms have better performance in imaging quality, less computational time and are vigorous.

The authors have also presented the particle swarm optimization algorithm for reconstructing the brain EIT images. Outcomes showed the error measures are limited within the define limits even under noisy conditions and the system is stable. They concluded that this PSO-EIT technique could be used in neurophysiological studies and to measure head geometry [15]. For head phantoms for intracranial hemorrhage (ICH) an EIT method is used to identify and image impedance variations. With and without a craniotomy, the authors have modeled the head phantoms of ICH. They have made two accurate head-shape models and a non-uniform resistivity distribution for brain EIT. To the head phantoms, they have inserted animal blood to replicate the ICH procedure and observed electrical impedance variations in real time with EIT. They have concluded from the injection of the blood region in one head phantom without the craniotomy that a growing impedance area appeared and on the other hand, in the second head phantom a reduced impedance area appeared. This shows that EIT is sensitive to impedance variations due to blood change. Instead, between two head phantoms, the varying trend showed in a contrasting way. This effect might be due to the variations in intracranial space and intracranial pressure. Therefore, for the treatment of ICH and for early diagnosis, EIT can be used. To solve the EIT inverse problem a differential evolution (DE) algorithm can be used [66]. For the forward problem, a FEM is chosen to determine the cost function. For real head model, this technique is applied for the 2D impedance reconstruction of brain section. Results showed that for the EIT problems the differential evolution algorithm is good in performance for obtaining high-quality reconstruction. Ying et al. [81] have reconstructed the real head model to examine the EIT images for the head. They have observed that because the skull forms a physical barrier and restricts the current flow it is the basic issue for the reconstruction of the head impedance image. Image distortion is produced due to this low conductivity region where conductivity variations are localized towards the image center. Because of deficient spatial resolution, simple global variations are identified and due to this reason, the purpose of imaging cannot be achieved. The electrodes were placed directly on to the heads of some animals instead of using scalp electrodes. This approach measures the clear impedance variations associated with neuronal activity, but this technique is not practical in medical applications for human beings. Nevertheless, if those restrictions are solved the outcomes are promising if image reconstruction and data acquisition methods are improved. In head impedance imaging, because of the high degree of non-linearity and deficiency of the perfect head models, the image reconstruction might be unsuccessful. Currently, a nonlinear difference imaging method has been presented to alleviate modeling error. This technique depends upon unconstrained modeling that permits tissue conductivity values to be unrealistically negative. Therefore, substantial image artifacts are probably conducted. In [82] two techniques of constrained modeling that can significantly reduce artifacts and increase localization performance are presented. The simulation result showed that the new images attain good localization performance as compared to those using unconstrained modeling

5.3. Breast Imaging

For detecting breast cancer, X-ray mammography is a convenient method but it is very costly to use regularly and might be dangerous if it is used regularly. The specificity of the mammography is not good but has a higher sensitivity. For regular breast scanning, EIT is a much more reliable and feasible technique. A major variance is noted in impedances between tumors and normal breast tissues. A 3D EIT system with 128 electrodes has been presented in which an electronic switching network controlled a data acquisition system. For calculating measured voltages and to remove the electrode impedance effect, a four-electrode method is used. For image reconstruction in EIT an iterative algorithm depends on the Distorted Born Iterative Method (DBIM) has been proven proficient and precise [83]. With the use of 16 electrodes internally present in a patient's breast-like finite element mesh, the authors have discovered a simulated anomaly (subject to specific conditions). Later, the experiments were done by adding two more rings of 16 electrodes to improve the resolution of the reconstructed images. They have also compared the model performance by using RMSE and Pearson's correlation coefficient [84]. An analysis of the performance of the EIT approach for

detecting breast cancer has been studied [3]. Two softwares called OCTAVE and EIDORS were used for simulation purposes. A comparison between three algorithms: prior Laplace, Newton's One-Step Error Reconstructor (NOSER), and Tikhonov have been made. Among the three-reconstruction algorithm, The NOSER algorithm achieved the best results due to the good classification performance metrics of proximity between neoplasms, as this factor alter the resolution of the reconstruction images generated based on the algorithm used [85]. Gowry et al. in [86] have directed their study into finding out whether high-speed EIT would be able to identify and distinguish the changes in conductivity with recurring Blood-volume changes and also to be able to determine the capability of the usage of these indications to extricate the benign regions from the malignant regions inside the breast. For briefly varying conductive, the initial validation was provided by EIT imaging of pulsating membranes (latex) that had been immersed in saline tubs. A study was carried out on 10 women with cancer and 9 without cancer (total 19) where they were imaged with EIT over series of their heartbeats (pulse-oximetry) in synchronization. The comparison of the malignant and benign regions of the breast was made by pertaining to the pulse oximeter signatures and the conductivity images of eight parameters. In seven of the eight parameters, critical differences amongst the benign and malignant regions of the breast [86]. By using the EIT technique the authors have recommended a reconstruction algorithm for the imaging of a breast tumor of a basic mammography geometry model [87]. By placing the electrodes on the highest point and the lowest point of the surfaces, they have modeled a four-sided geometry. For the homogenous conductivity distribution, a progressive model for the EIT imaging' complication is formulated and by using a phantom tank, the experimental setup is verified. For imaging a breast tumor, an algorithm (reconstruction) established on the linearization technique is also demonstrated. The results showed that for the phantom experiments the suggested reconstruction algorithm executes adequately [87]. In a similar experiment, a progressive model of the EIT imaging issue was presented. The experimental results verified the progressive model and highlighted that the predicted values complied with the measured electrode voltages. In addition, on the side of the electrodes, the effect of an unmodeled surface is also studied [88]. In [89] EIT has been used by the authors as a procedure for imaging breast cancer, for determining the admittivity dispersion within the breast. All the admittivity distributions obtained are much lesser in compressed breasts in EIT as compared to the previous experiments for imaging whole chest. They have projected a three-layered examining a progressive model of the breast: the highest layer of thin low admittivity, the lowest layers representing skin and a comparatively thicker high-admittivity middle layer portraying breast tissue. The authors have suggested a progressive solution to this layered portrayal relating this solution with the homogeneous case. They have concluded that the layered forward solution performed better reconstruction as compared to the homogeneous forward solution [90]. The authors have studied the use of EIT in comparison to the other techniques such as mammography (MMG); ultrasound (US) and biopsy. They have concluded that the EIT had 64.4% sensitivity and is recommended to be a promising method for scanning and detecting breast irregularities before breast self-examination. Nevertheless, MMG has to be done to confirm the analysis [89]. In [91] to get tissue impedance maps the authors have demonstrated the usage of adjustable higher density microelectrode arrays. Exact reconstruction in EIT is primarily based on spatial resolution and arrays to obtain tissue impedance maps. Flexible arrays with high density which are suitable to the surface of the breast can give high flexibility in the reconstruction of conductivity maps of advanced resolutions as compared to that have been formerly achieved [91].

5.4. Lung Imaging

Hua et al. [92] have demonstrated the usage of EIT imaging methods in the calculation of the resistivity of the Lungs in examining and detection of edema and apnea. In EIT, the current is injected into the patient by applying several electrodes and calculating border-line voltages to reform a cross-sectional image of internal resistivity distribution. They have presented a fast, simple method for observing and detecting apnea and edema. They demonstrated their method by human

experiments and simulations. They have concluded that the EIT imaging method will be more consistent as compared to the current impedance apnea monitoring technique, as they were monitoring the variations in the resistivity of the internal lung. They have suggested that more studies need to be done to validate this technique but that it performs better in the existence of motion artifact as compared to the traditional two-electrode impedance apnea monitoring technique. By taking a series of differential images, Chen et al. have proposed a system to observe human lung ventilation. The result of the experiments highlighted that the Multi Frequency (MF-EIT) system is a practical, reliable, appropriate and consistent technique of imaging human lung ventilation. It is possible to get an accurate reconstructed image in EIT by inserting previous data with reference to size constitution of the object. They used a commercial software tool COMSOL by including the prior information of human thorax to produce a physical model [93]. Alongside the ventilation of the lungs, the authors have presented a developed model too based on the experimental data. By including prior information, the imagery results of the ventilation of the lungs showed that EIT is a reliable procedure for medical analyses and monitoring and has the capabilities to use in the near future [93]. In [94] Shuai et al. have proposed a new three-dimensional swift real-time EIT system for imaging and detecting human lung that depends on the node back-projection algorithm with 64 electrodes. The findings indicated that the system contained the potential of reflecting impedance variations of the thorax reconstruction of the images amid a person's breathing. Zhao et al. have [95] proposed a better technique for EIT images for a lung area estimation (LAE). For patients with serious pulmonary diseases, LAE is an appropriate technique. They concluded that in EIT for the lung area estimation the LAE technique provides more reliable results as compared to the other different current techniques. Lee et al. produced an EIT-based wearable lung health-monitoring device. The system has an EIT integrated circuit (IC) that gives programmable current stimulation that is optimally controlled by the results of contact impedance monitoring. The data obtained is forwarded to the handheld mobile device and the lung EIT images of up to 20 frames/s real-time are reconstructed and displayed. The calculated lung air volume-ratio can be used as a pointer of the lung-health, and different other parameters that can be extracted to observe lung status from the lung EIT image obtained [96]. A similar device with less power consumption for lung ventilation monitoring is proposed [97]. The SoC with 32 electrodes on a belt-type EIT system gives dynamic images on the mobile device for lung ventilation. The device can reconstruct the imaginary and the real parts of the images with 97.3% of precision [97].

5.5. Osteography

In the majority of the scenarios, the healing of fractures is a simple procedure. However, in a few fractures, the union can be absent or even delayed. Plain film X-ray is usually used for the process of the assessment for the healing of the fractures but it is difficult. To envisage these fractures that are predisposed to vibration, non-union, ultrasound and mechanical stressing of the fracture, several techniques have already been employed. Some methods such as plain films indicate these fractures but they do it late in the process. The bone-scintigraphy technique is used to confirm an established non-union but their reports are based on the prognostic values and they are contradictory [98]. EIT indicates the electrical properties of the fractured and the normal limbs. In 1983, the very first human forearm image 'in vivo' was presented. Kulkarni and Ritchie [99] took the use of the EIT in the clinical side in six adult subjects. Across the fractured humerus, they have obtained the static images and compared it with the normal contra-lateral limb. Results from the images of the fresh fracture highlighted a drastic difference as compared to the contralateral normal limb. In addition, these images possibly showed edema represented by a huge area of low resistivity. In another case in a patient, a large area highlighted an increased resistivity, probably representing callus formation having a solidly united fracture. Another patient having an un-united fracture and it showed an area of low resistivity, most likely indicating fibrosis and edema. As union progresses, impedance osteography helps to indicate the existence of a fracture and variation in resistivity. Although the properties of a

recognized non-union are presented, still it needs to highlight whether, at an early stage, impedance osteography gives precise information for the non-union of the fractures.

6. Other Applications of EIT

Along with the EIT research, focus on impedance imaging in the physiological and medical field there has been significant research in the applications of process control. In 1980, Professor Maurice Beck presented impedance imaging as a process tomography and put his efforts into bringing the process and UK medical tomography groups on to the same platform. The joint venture and collaboration helped to promote these systems to develop in both research fields and resulted in the development of capacitive and inductive tomographies. The limitations are different in the process control as compared to that in medical since for liquids like oil and water, more than 200 frame rates per second need to be calculated at a time. The most relevant example is the calculations of the fast fluid flow in rigid pipes. Large fixed electrodes could be positioned around the pipe as capacitive tomography systems are practical in case of rigid pipes and the electrodes are not in contact with the flow of the liquid.

EIT is also used to identify small defects such as cracks or voids in metals and nondestructive testing for detecting corrosion. Since its early usage, the system has progressed remarkably with its technology as well as in its usage. Different researchers have discussed some other applications of the EIT. Kriz et al. [100] have outlined the application of EIT in non-destructive material testing. They have proposed an EIT-based reconstruction algorithm, demonstrating its usage for finding cracks in electrically conductive objects. The algorithm presented found to be proficient in finding a defect precisely.

Kai et al. [101] have presented a resistivity reconstruction technique that depends upon the magnetic detection of EIT to calculate the topology and breakpoints of the grounding grid. They have highlighted the efficiency of the proposed method by applying it on some a mathematical instance that confirms that the suggested approach can be implemented in finding the breakpoints and topology of the grounding grids.

7. Conclusions

EIT is progressively maturing as a tool for monitoring and imagining. It is relatively cheaper, non-invasive, and with no potential hazards. It has been widely used now in numerous biomedical and non-clinical applications. In this paper, steps to solve the EIT problem are briefly discussed; the artificial intelligence (AI) and evolutionary computational (EC) methods for solving the electrical tomography inverse problem are reviewed and clinical applications using electrical impedance tomography for imaging and function monitoring are discussed. Finally, we concluded that EIT is an open research area having the perspective to explore new AI and EC methods to solve this ill-conditioned problem. EIT is a next-generation imaging technique with huge potential to be used as a stable imaging modality in the future.

Author Contributions: Conceptualization, T.A.K. and S.H.L.; methodology, T.A.K.; formal analysis, T.A.K. and S.H.L.; investigation, T.A.K.; resources, T.A.K.; data curation, T.A.K. and S.H.L.; writing—original draft preparation, T.A.K.; writing—review and editing, T.A.K. and S.H.L.; visualization, T.A.K.; supervision, S.H.L.; project administration, S.H.L.

Funding: This research received no external funding.

Conflicts of Interest: The authors declare no conflict of interest.

References

1. Garg, D.; Goel, V. Design and development of Electrical Impedance Tomography (EIT) based System. *AIP Conf. Proc.* **2013**, *74*, 33–36. [[CrossRef](#)]

2. Boverman, G.; Isaacson, D.; Newell, J.C.; Saulnier, G.J.; Kao, T.J.; Amm, B.C.; Wang, X.; Davenport, D.M.; Chong, D.H.; Sahni, R.; et al. Efficient Simultaneous Reconstruction of Time-Varying Images and Electrode Contact Impedances in Electrical Impedance Tomography. *IEEE Trans. Biomed. Eng.* **2017**, *64*, 795–806. [[CrossRef](#)] [[PubMed](#)]
3. Song, X.; Xu, Y.; Dong, F.; Witte, R.S. An Instrumental Electrode Configuration for 3-D Ultrasound Modulated Electrical Impedance Tomography. *IEEE Sens. J.* **2017**, *17*, 8206–8214. [[CrossRef](#)] [[PubMed](#)]
4. Hu, J.Y.; Hu, J.G.; Lan, D.L.; Ming, J.L.; Zhou, Y.T.; Li, Y.W. Corrosion evaluation of the grounding grid in transformer substation using electrical impedance tomography technology. In Proceedings of the IECON 2017—43rd Annual Conference of the IEEE Industrial Electronics Society, Beijing, China, 29 October–1 November 2017; pp. 5033–5038.
5. Henderson, R.P.; Webster, J.G. An Impedance Camera for Spatially Specific Measurements of the Thorax. *IEEE Trans. Biomed. Eng.* **1978**, *BME-25*, 250–254. [[CrossRef](#)] [[PubMed](#)]
6. Balint, A.M.; Balint, Ş. Well posed problem in sense of Hadamard, for a source, produced acoustic perturbation propagation in a lined duct, carrying a gas flow. *Carpathian J. Math.* **2014**, *30*, 267–274.
7. De Freitas Barbosa, V.A.; Ramalho Ribeiro, R.; Rivalles Souza Feitosa, A.; Bezerra Araújo da Silva, V.L.; Diego Dias Rocha, A.; Covello de Freitas, R.; de Souza, R.E.; Pinheiro dos Santos, W. Reconstruction of Electrical Impedance Tomography Using Fish School Search, Non-Blind Search, and Genetic Algorithm. *arXiv* **2017**, arXiv:1712.00789.
8. Adler, A.; Guardo, R. A neural network image reconstruction technique for electrical impedance tomography. *IEEE Trans. Med. Imaging* **1994**, *13*, 594–600. [[CrossRef](#)]
9. Zhang, H.; Wang, L.; Zhou, Y.; Zhang, P.; Wu, J.; Li, Y. An Influence of the Noise on the Imaging Algorithm in the Electrical Impedance Tomography. *Open J. Biophys.* **2013**, *3*. [[CrossRef](#)]
10. Zhang, H.; Wang, H.; Zhou, Y.; Zhang, X. Research of electrical impedance tomography based on the Modified Particle Swarm Optimization. In Proceedings of the 2012 8th International Conference on Natural Computation, Chongqing, China, 29–31 May 2012; pp. 1216–1218.
11. Feitosa, A.R.S.; Ribeiro, R.R.; Barbosa, V.A.F.; de Souza, R.E.; dos Santos, W.P. Reconstruction of electrical impedance tomography images using chaotic ring-topology particle swarm optimization and non-blind search. In Proceedings of the 2014 IEEE International Conference on Systems, Man, and Cybernetics (SMC), San Diego, CA, USA, 5–8 October 2014; pp. 2618–2623.
12. Wang, P.; Xie, L.; Sun, Y. Application of PSO algorithm and RBF neural network in electrical impedance tomography. In Proceedings of the 2009 9th International Conference on Electronic Measurement & Instruments, Beijing, China, 16–19 August 2009; pp. 517–521.
13. Wang, H.; Xu, G.; Zhang, S.; Yan, W. Optimized Excitation Mode for Generalized Back Projection Algorithm in 3-D EIT. *IEEE Trans. Magn.* **2015**, *51*, 1–4. [[CrossRef](#)]
14. Liu, R.; Lin, M.; Rong, Z.; Li, K. Study on PSO-tGN algorithm of bio-electrical impedance tomography system. In Proceedings of the 11th World Congress on Intelligent Control and Automation, Shenyang, China, 29 June–4 July 2014; pp. 5808–5811.
15. Kumar, S.P.; Sraam, N.; Benakop, P.G.; Jinaga, B.C. Reconstruction of brain electrical impedance tomography images using particle swarm optimization. In Proceedings of the 2010 5th International Conference on Industrial and Information Systems, Mangalore, India, 29 July–1 August 2010; pp. 339–342.
16. Chen, M.-Y.; Hu, G.; He, W.; Yang, Y.-L.; Zhai, J.-Q. A Reconstruction Method for Electrical Impedance Tomography Using Particle Swarm Optimization. In Proceedings of the International Conference on Life System Modeling and Simulation, Wuxi, China, 17–20 September 2010; pp. 342–350. [[CrossRef](#)]
17. Martin, S.; Choi, C.T.M. *Electrical Impedance Tomography: A Reconstruction Method Based on Neural Networks and Particle Swarm Optimization*; Springer: Cham, Switzerland, 2015; pp. 177–179.
18. Choi, C.T.M. An Optimal Training Method for Artificial Neural Networks in Electrical Impedance Tomography. Presented at Electrical Impedance Tomography, Neuchâtel, Switzerland, 2–5 June 2015; p. 12.
19. Lee, B.A.; Kim, B.S.; Ko, M.S.; Kim, K.Y.; Kim, S.I.N. Electrical resistance imaging of two-phase flow with a mesh grouping technique based on particle swarm optimization. *Nucl. Eng. Technol.* **2014**, *46*, 109–116. [[CrossRef](#)]
20. Wang, P.; Lin, J.S.; Wang, M. An image reconstruction algorithm for electrical capacitance tomography based on simulated annealing particle swarm optimization. *J. Appl. Res. Technol.* **2015**, *13*, 197–204. [[CrossRef](#)]

21. Ijaz, U.Z.; Khambampati, A.K.; Kim, M.C.; Kim, S.; Lee, J.S.; Kim, K.Y. Particle Swarm Optimization Technique for Elliptic Region Boundary Estimation In Electrical Impedance Tomography. *AIP Conf. Proc.* **2007**, *914*, 896–901. [[CrossRef](#)]
22. Chen, M.-Y.; Yang, Y.-L.; He, W.; Zhang, C.-Y.; Li, B. Image reconstruction of electrical impedance tomography based on particle swarm optimization algorithm. *J. Chongqing Univ.* **2011**, *34*, 82–87.
23. Zhang, H.; Zhang, X.; Ji, J.; Yao, Y. Electromagnetic imaging of the 2-D media based on Particle Swarm Algorithm. In Proceedings of the 2010 Sixth International Conference on Natural Computation, Yantai, China, 10–12 August 2010; pp. 262–265.
24. Jian, C.Y.S.F.Z. A Novel Gray Boundary Compensation Algorithm for Electrical Capacitance Tomography System Based on Adaptive Particle Swarm Weight. *J. Harbin Univ. Sci. Technol.* **2010**, *1*, 44–49.
25. Sun, Q.; Shi, T. Sensors Structure Optimization of ECT Based on RBF Neural Network and PSO. *Control Instrum in Chem. Ind.* **2009**, *2*.
26. Zhang, Y.-J.; Chen, D.-Y. Algebraic neural network image reconstruction algorithm for electrical resistance tomography. *Comput. Eng. Appl.* **2009**, *4*, 16–23.
27. Cai, Q.; Ma, N.; Su, X.; Wang, Y. Using BP neural network in electrical capacitance tomography. *Wuhan Univ. J. (Nat. Sci. Ed.)* **1997**, *43*, 107–112.
28. Zhang, L.; Hu, H.; Chen, D.-Y. An Improved Image Reconstruction Algorithm of Electrical Capacitance Tomography Based on RBF Neural Network. *J. Harbin Univ. Sci. Technol.* **2008**, *2*, 5–8.
29. Wei, Y.; Zhao, J.; Wang, S.; Lu, Z. Research of the Image Reconstruction Algorithm for Electrical Resistance Tomography (ERT) Based on RBF Neural Network. *Chin. J. Sci. Instrum.* **2001**, *1*, 369–371.
30. Bao, P.-Q.; Li, Y.; Zhang, L.-Y.; Guo, H. Image Reconstruction Algorithm Based on RBF Neural Networks for Electrical Capacitance Tomography. *J. Harbin Univ. Sci. Technol.* **2008**, *4*, 23–26.
31. Hua, X.; Hu, G.; He, H.; Bao, Z. Research of Two BP Networks for Two-Phase Flow Electrical Capacitance Tomography. *Acta Metrol. Sin.* **1998**, *4*, 34–44.
32. Zhang, X.; Chen, X.; Hu, H.-L. An ECT image reconstruction algorithm using BP neural network and median filter. *Autom. Instrum.* **2010**, *2*, 7–15.
33. Zhao, J.; Xu, Q.; Zhang, J.; Li, T. RBF Neural Network Application to ECT Image Reconstruction. *Comput. Eng. Appl.* **2003**, *2*, 215–218.
34. Hu, H.; Chan, C.; Bai, T. ECT Image Reconstruction Algorithm by RBF Network and Wavelet Transform. *J. Xi'an Jiaotong Univ.* **2010**, *3*, 1–5.
35. Yan, H.; Zhu, A.-H.; Wang, B.; Zhou, Q. ECT image reconstruction based on RBF neural networks. *J. Shenyang Univ. Technol.* **2007**, *5*, 20–27.
36. Zhao, J.; Fu, W.; Li, T.; Liang, J. Image Reconstruction New Algorithm for Electrical Capacitance Tomography. *Comput. Eng. Appl.* **2004**, *30*, 54–57.
37. Xiao Hua He Huiling Hu Guangli Bao Zongti. Application Research on the Electrical Capacitance Tomography Using Multi-layer Neural Network. *J. Circuits Syst.* **1998**, *1*, 12–18.
38. Zhang, L.; Wang, H.-X. Image Reconstruction Algorithm for Electrical Capacitance Tomography Based on Wavelet Neural Networks. *Proc. CSEE* **2008**, *10*, 42–54.
39. Kłosowski, G.; Rymarczyk, T. Using neural networks and deep learning algorithms in electrical impedance tomography. *Informatyka, Automatyka, Pomiary w Gospodarce i Ochronie Środowiska* **2017**, *7*, 99–102. [[CrossRef](#)]
40. Marashdeh, Q.; Warsito, W.; Liang-Shih, F.; Teixeira, F.L. Nonlinear forward problem solution for electrical capacitance tomography using a feed-forward neural network. *IEEE Sens. J.* **2006**, *6*, 441–449. [[CrossRef](#)]
41. Ratajewicz-Mikolajczak, E.; Shirkoohi, G.H.; Sikora, J. Two ANN reconstruction methods for electrical impedance tomography. *IEEE Trans. Magn.* **1998**, *34*, 2964–2967. [[CrossRef](#)]
42. Lampinen, J.; Vehtari, A.; Leinonen, K. Using Bayesian Neural Network to Solve the Inverse Problem in Electrical Impedance Tomography. In Proceedings of the 11th Scandinavian Conference on Image Analysis (SCIA'99), Strømfjord, Greenland, 7–11 June 1999.
43. Stasiak, M.; Sikora, J.; Filipowicz, S.F.; Nita, K. Principal component analysis and artificial neural network approach to electrical impedance tomography problems approximated by multi-region boundary element method. *Eng. Anal. Bound. Elem.* **2007**, *31*, 713–720. [[CrossRef](#)]
44. Marashdeh, Q.; Warsito, W.; Fan, L.S.; Teixeira, F.L. A nonlinear image reconstruction technique for ECT using a combined neural network approach. *Meas. Sci. Technol.* **2006**, *17*, 2097. [[CrossRef](#)]

45. Filho, R.G.N.S.; Campos, L.C.D.; dos Santos, R.W.; Barra, L.P.S. *Artificial Neural Networks Ensemble Applied to the Electrical Impedance Tomography Problem to Determine the Cardiac Ejection Fraction*; Springer: Cham, Switzerland, 2014; pp. 734–741.
46. Michalikova, M.; Abed, R.; Prauzek, M.; Koziorek, J. Image reconstruction in electrical impedance tomography using a neural network. In Proceedings of the 2014 Cairo International Biomedical Engineering Conference (CIBEC), Giza, Egypt, 11–13 December 2014; pp. 39–42.
47. Hrabuska, R.; Prauzek, M.; Venclikova, M.; Konecny, J. Image Reconstruction for Electrical Impedance Tomography: Experimental Comparison of Radial Basis Neural Network and Gauss-Newton Method. *IFAC-PapersOnLine* **2018**, *51*, 438–443. [[CrossRef](#)]
48. Lu, X.; Zhou, M. *Intelligent Algorithms and Their Application in Electrical Impedance Tomography*; Springer: Cham, Switzerland, 2016; pp. 35–43.
49. Xiao, L.; Wang, H. Optimization of node numbering in ERT finite element mesh based on improved genetic algorithm. *Comput. Eng. Appl.* **2011**, *47*, 20–22.
50. Chen, D.-Y.; Zheng, G.-B.; Yu, X.-Y.; Sun, L.-Q. Image reconstruction algorithm based on genetic algorithms for two-phase flow electrical capacitance tomography system. *Electr. Mach. Control* **2003**, *7*, 207–211.
51. Olmi, R.; Bini, M.; Priori, S. A genetic algorithm approach to image reconstruction in electrical impedance tomography. *IEEE Trans. Evolut. Comput.* **2000**, *4*, 83–88. [[CrossRef](#)]
52. Kim, H.-C.; Boo, C.-J.; Kang, M.-J. *Image Reconstruction Using a Genetic Algorithm in Electrical Impedance Tomography*; Springer: Berlin/Heidelberg, Germany, 2006; pp. 938–945.
53. Rolnik, V.P.; Selegheim, P., Jr. A specialized genetic algorithm for the electrical impedance tomography of two-phase flows. *J. Braz. Soc. Mech. Sci. Eng.* **2006**, *28*, 378–389. [[CrossRef](#)]
54. Carosio, G.; Rolnik, V.; Selegheim, P. Improving Efficiency in Electrical Impedance Tomography Problem by Hybrid Parallel Genetic Algorithm and a Priori Information. 2007. Available online: https://www.researchgate.net/publication/228945026_Improving_efficiency_in_electrical_impedance_tomography_problem_by_hybrid_parallel_genetic_algorithm_and_a_priori_information_In_editor (accessed on 25 April 2019).
55. Cheng, K.-S.; Chen, B.-H.; Tong, H.-S. Electrical impedance image reconstruction using the genetic algorithm. In Proceedings of the 18th Annual International Conference of the IEEE Engineering in Medicine and Biology Society, Amsterdam, The Netherlands, 31 October–3 November 1996; Volume 762, pp. 768–769.
56. Chen, Z.; Zhao, B.; Wang, H. New landweber method based tikhonov for image reconstruction for ECT. *Electron. Meas. Technol.* **2007**, *30*, 61–63.
57. Min, X.X.H. LM algorithm for electromagnetic tomography image reconstruction. Presented at the Ninth Youth Academic Conference of China Instrument and Control Society, Hefei, China, 1–2 October 2007.
58. Chen, D.Y.; Li, L.; Hu, H.-T. Image Reconstruction Algorithm Based on Iterated Tikhonov Regularization for Electrical Capacitance Tomography. *J. Harbin Univ. Sci. Technol.* **2009**, *1*, 1–3.
59. Liu, H.-Y.; Chen, D.-Y.; Li, M.-Z. Image Reconstruction Algorithms of Electrical Capacitance Tomography Based on Support Vector Machine. *J. Harbin Univ. Sci. Technol.* **2006**, *5*, 10–18.
60. Jing, L.; Meng, S.; Dong, X.; Shi, L. Image reconstruction algorithm for electrical capacitance tomography based on pre-optimization transition. *Chin. J. Sci. Instrum.* **2007**, *28*, 394.
61. Jing, L.; Shi, L.; Li, Z. Image reconstruction iteration algorithm based on 1-norm for electrical capacitance tomography. *Chin. J. Sci. Instrum.* **2007**, *29*, 1355–1358.
62. He, S.-J.; Han, Y.-H.; Li, Z.-Y.; Gao, Y.; Li, H. Study of Image Reconstruction Algorithm Based on Active Filter Linear Back Projection Method. *Henan Sci.* **2006**, *7*, 26–34.
63. Kim, H.; Kim, K.Y.; Park, J.W.; Lee, H.J. Electrical impedance tomography reconstruction algorithm using extended Kalman filter. In Proceedings of the 2001 IEEE International Symposium on Industrial Electronics Proceedings (Cat. No.01TH8570), Pusan, Korea, 12–16 June 2001; Volume 1673, pp. 1677–1681.
64. Trigo, F.C.; Gonzalez-Lima, R.; Amato, M.B.P. Electrical impedance tomography using the extended Kalman filter. *IEEE Trans. Biomed. Eng.* **2004**, *51*, 72–81. [[CrossRef](#)]
65. Dos Santos, W.; Barbosa, V.; Emmanuel de Souza, R.; Ribeiro, R.; Feitosa, A.; Silva, V.; Ribeiro, D.; Covello de Freitas, R.; Paschoal de Medeiros Lima, M.; Soares, N.; et al. Image Reconstruction of Electrical Impedance Tomography Using Fish School Search and Differential Evolution. In *Critical Developments and Applications of Swarm Intelligence*; IGI Global: Hershey, PA, USA, 2018. [[CrossRef](#)]

66. Li, Y.; Rao, L.; He, R.; Xu, G.; Wu, Q.; Ge, M.; Yan, W. Image reconstruction of EIT using differential evolution algorithm. In Proceedings of the 25th Annual International Conference of the IEEE Engineering in Medicine and Biology Society, Cancun, Mexico, 17–21 September 2003; Volume 1012, pp. 1011–1014.
67. Vauhkonen, M.; Karjalainen, P.A.; Kaipio, J.P. A Kalman filter approach to track fast impedance changes in electrical impedance tomography. *IEEE Trans. Biomed. Eng.* **1998**, *45*, 486–493. [[CrossRef](#)]
68. Liu, S.; Jia, J. Sequential EIT frame reconstruction exploiting spatiotemporal correlation. In Proceedings of the 19th International Conference on Biomedical Applications of Electrical Impedance Tomography (EIT 2018), Edinburgh, UK, 11–13 June 2018.
69. Liu, S.; Jia, J.; Zhang, Y.D.; Yang, Y. Image Reconstruction in Electrical Impedance Tomography Based on Structure-Aware Sparse Bayesian Learning. *IEEE Trans. Med. Imaging* **2018**, *37*, 2090–2102. [[CrossRef](#)]
70. Liu, S.; Wu, H.; Huang, Y.; Yang, Y.; Jia, J. Accelerated Structure-Aware Sparse Bayesian Learning for 3D Electrical Impedance Tomography. *IEEE Trans. Ind. Inform.* **2019**. [[CrossRef](#)]
71. Liu, S.; Jia, J.; Yang, Y. Image reconstruction algorithm for electrical impedance tomography based on block sparse Bayesian learning. In Proceedings of the 2017 IEEE International Conference on Imaging Systems and Techniques (IST), Beijing, China, 18–20 October 2017; pp. 1–5.
72. Sikora, R.; Giza, Z.; Filipowicz, F.; Sikora, J. The bell function approximation of material coefficients distribution in the electrical impedance tomography. *IEEE Trans. Magn.* **2000**, *36*, 1023–1026. [[CrossRef](#)]
73. Chen, J.D.; Lin, Z.; McCallum, R.W. Noninvasive feature-based detection of delayed gastric emptying in humans using neural networks. *IEEE Trans. Biomed. Eng.* **2000**, *47*, 409–412. [[CrossRef](#)] [[PubMed](#)]
74. Avill, R.; Mangnall, Y.F.; Bird, N.C.; Brown, B.H.; Barber, D.C.; Seagar, A.D.; Johnson, A.G.; Read, N.W. Applied potential tomography. A new noninvasive technique for measuring gastric emptying. *Gastroenterology* **1987**, *92*, 1019–1026. [[CrossRef](#)]
75. Mangnall, Y.F.; Baxter, A.J.; Avill, R.; Bird, N.C.; Brown, B.H.; Barber, D.C.; Seagar, A.D.; Johnson, A.G.; Read, N.W. Applied potential tomography: A new non-invasive technique for assessing gastric function. *Clin. Phys. Physiol. Meas.* **1987**, *8* (Suppl. A), 119–129. [[CrossRef](#)] [[PubMed](#)]
76. Lamont, G.L.; Wright, J.W.; Evans, D.F.; Kapila, L. An evaluation of applied potential tomography in the diagnosis of infantile hypertrophic pyloric stenosis. *Clin. Phys. Physiol. Meas.* **1988**, *9* (Suppl. A), 65–69. [[CrossRef](#)]
77. Huerta-Franco, M.R.; Vargas-Luna, M.; Montes-Frausto, J.B.; Flores-Hernández, C.; Morales-Mata, I. Electrical bioimpedance and other techniques for gastric emptying and motility evaluation. *World J. Gastrointest. Pathophysiol.* **2012**, *3*, 10–18. [[CrossRef](#)] [[PubMed](#)]
78. Ren, C.S.; Wang, Y.; Zhao, S. Electrical impedance tomography measuring gastric emptying and gastric motility. *World Chin. J. Digestol.* **2008**, *16*, 799–805. [[CrossRef](#)]
79. Boone, K.; Lewis, A.M.; Holder, D.S. Imaging of cortical spreading depression by EIT: Implications for localization of epileptic foci. *Physiol. Meas.* **1994**, *15* (Suppl. 2a), A189–A198. [[CrossRef](#)] [[PubMed](#)]
80. Holder, D. Electrical impedance tomography of brain function: Overview and technical considerations. In Proceedings of the International Conference on Electrical Bioimpedance, Oslo, Denmark, 17–21 June 2001; pp. 467–472.
81. Xu, G.; Yang, Q.; Li, Y.; Wu, Q.; Yan, W. The electrical properties of real head model based on electrical impedance tomography (EIT). In Proceedings of the 25th Annual International Conference of the IEEE Engineering in Medicine and Biology Society (IEEE Cat. No.03CH37439), Cancun, Mexico, 17–21 September 2003; Volume 991, pp. 994–997.
82. Ouyyornkochagorn, T. Constrained modeling for image reconstruction in the application of Electrical Impedance Tomography to the head. In Proceedings of the 2017 IEEE 14th International Symposium on Biomedical Imaging (ISBI 2017), Melbourne, Australia, 18–21 April 2017; pp. 548–551.
83. Gang, Y.; Lim, K.H.; George, R.; Ybarra, G.; Joines, W.T.; Liu, Q.H. A 3D EIT system for breast cancer imaging. In Proceedings of the 3rd IEEE International Symposium on Biomedical Imaging: Nano to Macro, Arlington, VA, USA, 6–9 April 2006; pp. 1092–1095.
84. Abdi, M.; Liatsis, P. EIT in Breast Cancer Imaging: Application to Patient-Specific Forward Model. In Proceedings of the 2011 Developments in E-systems Engineering, Dubai, UAE, 6–8 December 2011; pp. 56–61.
85. Ferreira, H.R.; Bustos, H.I.A.; Figuerola, W.B. Simulation inverse problems of reconstruction of image data using patterned electrical impedance tomography female breast. In Proceedings of the 2014 IEEE 16th International Conference on e-Health Networking, Applications and Services (Healthcom), Natal, Brazil, 15–18 October 2014; pp. 1–6.

86. Gowry, B.; Shahriman, A.B.; Paulraj, M. Electrical bio-impedance as a promising prognostic alternative in detecting breast cancer: A review. In Proceedings of the 2015 2nd International Conference on Biomedical Engineering (ICoBE), Penang, Malaysia, 30–31 March 2015; pp. 1–6.
87. Choi, M.H.; Kao, T.J.; Isaacson, D.; Saulnier, G.J.; Newell, J.C. A Reconstruction Algorithm for Breast Cancer Imaging with Electrical Impedance Tomography in Mammography Geometry. *IEEE Trans. Biomed. Eng.* **2007**, *54*, 700–710. [[CrossRef](#)]
88. Choi, M.H.; Kao, T.J.; Isaacson, D.; Saulnier, G.J.; Newell, J.C. A simplified model of mammography geometry for breast cancer imaging with electrical impedance tomography. In Proceedings of the 26th Annual International Conference of the IEEE Engineering in Medicine and Biology Society, San Francisco, CA, USA, 1–5 September 2004; pp. 1310–1313.
89. Zain, N.M.; Kanaga, K.C.; Sharifah, M.I.A.; Suraya, A.; Latar, N.H. Study of Electrical Impedance Tomography as a primary screening technique for breast cancer. In Proceedings of the 2014 IEEE Conference on Biomedical Engineering and Sciences (IECBES), Kuala Lumpur, Malaysia, 8–10 December 2014; pp. 220–224.
90. Kulkarni, R.; Boverman, G.; Isaacson, D.; Saulnier, G.; Newell, J.C. Layered Model for Breasts in Electrical Impedance Tomography. In Proceedings of the 2007 29th Annual International Conference of the IEEE Engineering in Medicine and Biology Society, Lyon, France, 22–26 August 2007; pp. 4150–4153.
91. Campisi, M.S.; Barbre, C.; Chola, A.; Cunningham, G.; Woods, V.; Viventi, J. Breast cancer detection using high-density flexible electrode arrays and electrical impedance tomography. In Proceedings of the 2014 36th Annual International Conference of the IEEE Engineering in Medicine and Biology Society, Chicago, IL, USA, 26–30 August 2014; pp. 1131–1134.
92. Woo, E.J.; Hua, P.; Webster, J.G.; Tompkins, W.J. Measuring lung resistivity using electrical impedance tomography. *IEEE Trans. Biomed. Eng.* **1992**, *39*, 756–760. [[CrossRef](#)]
93. Chen, X.; Wang, H.; Shi, X.; Yan, Y.; Cui, Z. Lung Ventilation Monitoring Incorporating Prior Information by Electrical Impedance Tomography. In Proceedings of the 2008 IEEE Instrumentation and Measurement Technology Conference, Victoria, BC, Canada, 12–15 May 2008; pp. 1531–1536.
94. Zhang, S.; Xu, G.; Zhang, J.; Wang, H.; Geng, D.; Shen, X.; Yan, W.; Liu, F.; Yang, X. Three dimensional detection and imaging for human lung based on node back-projection algorithm with a 64 electrodes EIT system. In Proceedings of the Digests of the 2010 14th Biennial IEEE Conference on Electromagnetic Field Computation, Chicago, IL, USA, 9–12 May 2010.
95. Zhao, Z.; Moller, K.; Steinmann, D.; Guttman, J. Determination of Lung Area in EIT Images. In Proceedings of the 2009 3rd International Conference on Bioinformatics and Biomedical Engineering, Beijing, China, 11–13 June 2009; pp. 1–4.
96. Hong, S.; Lee, J.; Yoo, H.J. Wearable lung-health monitoring system with electrical impedance tomography. In Proceedings of the 2015 37th Annual International Conference of the IEEE Engineering in Medicine and Biology Society (EMBC), Milan, Italy, 25–29 August 2015; pp. 1707–1710.
97. Hong, S.; Lee, J.; Bae, J.; Yoo, H.J. A 10.4 mW Electrical Impedance Tomography SoC for Portable Real-Time Lung Ventilation Monitoring System. *IEEE J. Solid-State Circuits* **2015**, *50*, 2501–2512. [[CrossRef](#)]
98. Dell’Osa, A. Bone Electrical Impedance and Tomographic Reconstruction of Fracture Detection: A Review. In Proceedings of the II Latin American Conference on Bioimpedance, Montevideo, Uruguay, 30 September–2 October 2015; pp. 12–15. [[CrossRef](#)]
99. Ritchie, I.K.; Kulkarni, V. Impedance osteography: Clinical applications of a new method of imaging fractures. *J. Biomed. Eng.* **1990**, *12*, 369–374. [[CrossRef](#)]
100. Kriz, T.; Dusek, J. Electrical impedance tomography in the testing of material defects. In Proceedings of the 2017 Progress In Electromagnetics Research Symposium-Spring (PIERS), St. Petersburg, Russia, 22–25 May 2017; pp. 90–94.
101. Liu, K.; Yang, F.; Zhang, S.; Zhu, L.; Hu, J.; Wang, X.; Ullah, I. Research on Grounding Grids Imaging Reconstruction Based on Magnetic Detection Electrical Impedance Tomography. *IEEE Trans. Magn.* **2018**, *54*, 1–4. [[CrossRef](#)]

